Pharm Res (2013) 30:447–457
DOI 10.1007/s11095-012-0890-6

RESEARCH PAPER

Effect of the Fluoroquinolone Antibacterial Agent DX-619 on the Apparent Formation and Renal Clearances of 6β-Hydroxycortisol, an Endogenous Probe for CYP3A4 Inhibition, in Healthy Subjects

Yuichiro Imamura • Nobuyuki Murayama • Noriko Okudaira • Atsushi Kurihara • Katsuhisa Inoue • Hiroaki Yuasa • Takashi Izumi • Hiroyuki Kusuhara • Yuichi Sugiyama

Received: 22 June 2012 / Accepted: 13 September 2012 / Published online: 17 October 2012

ABSTRACT

Purpose To examine the effect of the fluoroquinolone DX-619 on CYP3A4 and urinary excretion of 6β-hydroxycortisol, an endogenous probe of hepatic CYP3A4 activity, in healthy subjects.

Methods The effect of DX-619 on CYP3A4 was examined in human liver microsomes. The apparent formation and renal clearance of 6β-hydroxycortisol ($CL_{6\beta-OHF}$ and $CL_{renal,6\beta-OHF}$, respectively) were determined in placebo- and DX-619-treated subjects. 6β-hydroxycortisol uptake was determined in HEK293 cells expressing OAT1, OAT3, OCT2, MATE1, and MATE2-K.

Results DX-619 was a mechanism-based inhibitor of CYP3A4, with K_I and k_{inact} of 67.9 ± 7.3 μmol/l and 0.0730 ± 0.0033 min^{-1}, respectively. Pharmacokinetic simulation suggested *in vivo* relevance of CYP3A4 inhibition by DX-619. $CL_{6\beta-OHF}$ and $CL_{renal,6\beta-OHF}$ were decreased 72% and 70%, respectively, on day 15 in DX-619-treated group compared with placebo ($P < 0.05$). 6β-hydroxycortisol was a substrate of OAT3 ($K_m = 183 \pm 25$ μmol/l), OCT2, MATE1, and MATE2-K. Maximum unbound concentration of DX-619 (9.1 ± 0.4 μmol/l) was above K_i of DX-619 for MATE1 (4.32 ± 0.79 μmol/l).

Conclusions DX-619 caused a moderate inhibition of hepatic CYP3A4-mediated formation and significant inhibition of MATE-mediated efflux of 6β-hydroxycortisol into urine. Caution is needed in applying $CL_{6\beta-OHF}$ as an index of hepatic CYP3A4 activity without evaluating $CL_{renal,6\beta-OHF}$.

KEY WORDS CYP3A4 · drug-drug interaction · mechanism-based inhibition (MBI) · renal drug transporter · tubular secretion

ABBREVIATIONS

6β-OHF	6β-hydroxycortisol
AUC	area under the concentration-time curve
BBM	brush border membrane
C_{max}	maximum plasma concentration
CYP	cytochrome P450
ES	estrone-3-sulfate
HEK	human embryonic kidney
HLM	human liver microsomes
k_{deg}	degradation rate constant (turnover rate constant) of liver CYP3A4
MRM	multiple reaction monitoring
PAH	para-aminohippuric acid
TEA	tetraethylammonium

Y. Imamura • N. Murayama • N. Okudaira • A. Kurihara • T. Izumi
Drug Metabolism & Pharmacokinetics Research Laboratories, R&D Division Daiichi Sankyo Co., Ltd
1-2-58, Hiromachi, Shinagawa-ku, Tokyo 140-8710, Japan

K. Inoue • H. Yuasa
Department of Biopharmaceutics
Graduate School of Pharmaceutical Sciences
Nagoya City University
3-1 Tanabe-dori, Mizuho-ku, Nagoya 467-8603, Japan

H. Kusuhara
Laboratory of Molecular Pharmaceutics
Graduate School of Pharmaceutical Sciences
University of Tokyo
7-3-1, Hongo, Bunkyo-ku, Tokyo 113-0033, Japan

Y. Sugiyama (✉)
Sugiyama Laboratory, RIKEN Innovation Center
Research Cluster for Innovation, RIKEN
The Institute of Physical and Chemical Research
1-6 Suehiro-cho, Tsurumi-ku,
Yokohama City, Kanagawa 230-0045, Japan
e-mail: ychi.sugiyama@riken.jp

INTRODUCTION

Pharmacokinetic drug-drug interactions (DDIs) that cause accumulation of victim drugs in the body can potentiate the pharmacological effect or cause adverse reactions (1). To avoid severity, the magnitude of inhibition of drug metabolizing enzymes, and transporters are evaluated during drug discovery. In addition to the probe drugs, endogenous compounds have been employed to evaluate the magnitude interaction involving drug metabolizing enzymes and transporters *in vivo*. The advantage of this approach is the capability to suggest *in vivo* relevance of DDIs without administrating probe drugs in the subjects. However, its rationale as probe substrate is generally based on the association studies where the effect of inducers or inhibitors of metabolic enzymes and transporters on the pharmacokinetics of the endogenous probes was examined. Unlike probe drugs, the basic pharmacokinetics of the endogenous substrate, such as total body clearance and contribution of metabolic enzymes and transporters to the elimination from the systemic circulation, is not available.

6β-Hydroxycortisol (6β-OHF) is produced from cortisol by hepatic cytochrome P450 3A4 (CYP3A4) (2,3), one of the major drug metabolizing enzymes in the liver and small intestine (4). Since both cortisol and 6β-OHF are excreted into the urine (5), the ratio of concentration of 6β-OHF to cortisol in the urine ($R_{6\beta-OHF/F}$) was initially used as a conventional noninvasive measure of CYP3A activity (6). The apparent endogenous cortisol 6β-hydroxylation clearance ($CL_{6\beta-OHF}$) (calculated from the amount of urinary 6β-OHF excretion divided by the AUC of cortisol) has been proposed as an improved index for phenotyping the *in vivo* CYP3A activity since $R_{6\beta-OHF/F}$ is influenced by the inhibition of the renal elimination of cortisol by the test drugs (7,8). $CL_{6\beta-OHF}$ was significantly decreased by 51% in healthy subjects given a single dose of itraconazole (400 mg) (3) and by 51% on day 1, and 53–61% on day 2–6 in healthy subjects given a repeated administration of clarithromycin (200 mg, b.i.d, for 6 days) (7,8).

DX-619 (Fig. 1) is a novel des-fluoro(6)-quinolone antibacterial agent which exhibits a potent antibacterial effect *in vitro* and *in vivo* against multidrug-resistant staphylococci (9).

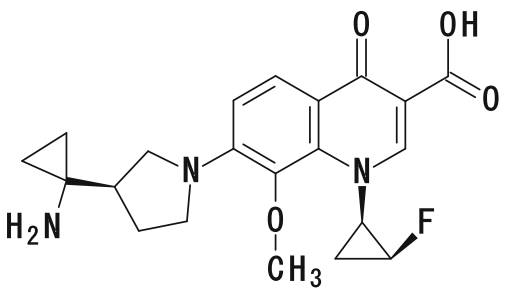

Fig. 1 Structure of DX-619.

Preliminary *in vitro* screening uncovered that DX-619 is a mechanism-based inhibitor of CYP3A4. Mechanism-based inhibition (MBI) is an irreversible type of inhibition for a metabolizing enzyme attributable to the covalent binding of reactive metabolites produced by the enzyme, and thus, the inhibition lasts even after the inhibitors are completely removed from the body. The primary purpose of this study is evaluation of the *in vivo* relevance of CYP3A4 inhibition by DX-619. We determined the $CL_{6\beta-OHF}$ using phase I samples from healthy subjects (eight males and one female) who had received a single dose of DX-619 (given by intravenous infusion of 1200 mg for 2 h), and then 48 h after the initial dose, received multiple dosings (1200 mg of DX-619 q.d. on day 3–15). The second purpose of this study was to evaluate the effect of DX-619 on the renal elimination of 6β-OHF. Measurement of $CL_{6\beta-OHF}$ as index of hepatic CYP3A4 inhibition relies on the assumption that 6β-OHF is mainly cleared renally, or that inhibitors do not inhibit urinary excretion and metabolism of 6β-OHF. Nevertheless, this has not been investigated in humans. Since OAT3 and P-glycoprotein was reported to transport cortisol as substrate *in vitro* (10,11), it is possible that 6β-OHF undergoes the transporter-mediated tubular secretion which provides the interaction site with drugs. We reported that DX-619 is an inhibitor of renal organic cation transporters (OCT2, MATE1 and MATE2-K), at the dosage. (12) This study investigated the renal elimination mechanisms of 6β-OHF in humans, and examined the effect of DX-619 on the renal clearance of 6β-OHF.

MATERIALS AND METHODS

Chemicals and Reagents

Cortisol, 6β-OHF, probenecid, quinidine, pyrimethamine, carbenoxolone and 6α-methylprednisolone were purchased from Sigma-Aldrich (St. Louis, MO). GF120918 was purchased from Toronto Research Chemicals Inc. (Ontario, Canada). DX-619 and deuterium-labeled DX-619 (d_3-DX-619) were synthesized in Daiichi Sankyo Co., Ltd. (Tokyo, Japan). Pooled HLM and human CYP3A4 supersomes were purchased from BD Gentest (Woburn, MA). All other reagents were of analytical grade and commercially obtained.

MBI of Midazolam 1'-hydroxylation by DX-619 in HLM

MBI of midazolam 1'-hydroxylation in HLM and CYP3A4 supersome were examined as reported previously (13) to determine the kinetic parameters. Kinetic parameters for enzyme inactivation, K_I and k_{inact}, which represents the apparent dissociation constant between CYP3A4 and DX-

619 and the maximum inactivation rate constant, respectively, were determined as described previously (13). Briefly, the natural logarithm of percent activity remaining was plotted against the preincubation times (0, 5, 10, 20 and 30 min) for each concentration (0, 12.5, 25, 50, 100 and 200 μmol/l) of DX-619. The slope from the linear regression analysis gave the observed inactivation rate constant (k_{obs}) and the inhibitor concentration (I) were fitted into the following expression using WinNonlin Professional ver 5.0 (Pharsight Corporation, Mountain View, CA).

$$k_{obs} = k_{inact} \cdot I/(K_I + I) \quad (1)$$

The unbound fraction of DX-619 ($f_{u,HLM}$) in the incubation media containing HLM (1 mg/ml) was determined by the ultrafiltration method using himac CS 150 GXII (Hitachi Koki Co., Ltd., Tokyo, Japan).

Simulation of the *In Vivo* CYP3A Activities during DX-619 Administration

The following differential equations for active CYP3A in the liver (E_{act}) have been cited from a previous report (14).

$$dE_{act}/dt = -\left(k_{inact} \cdot E_{act} \cdot f_{p,\mathrm{DX-619}} \cdot C_{p,\ \mathrm{DX-619}}\right)/ \left(K_I + f_{p,\ \mathrm{DX-619}} \cdot C_{p,\ \mathrm{DX-619}}\right).+k_{\mathrm{deg}}(E_0 - E_{act}) \quad (2)$$

where E_0, k_{deg}, $f_{p,DX-619}$, and $C_{p,\ DX-619}$ represent the initial value of hepatic CYP3A4 content, degradation rate constant of liver CYP3A, unbound fraction of DX-619 in plasma (29–34%, (12)), and DX-619 concentration in the plasma, respectively. It was assumed that the synthesis rate of liver CYP3A4 is assumed to be equal to the initial degradation date ($k_{deg} \cdot E_0$), and that DX-619 did not affect the synthesis rate, and k_{deg}. Due to the low liver extraction ratio (E_h) of DX-619 (0.10), the unbound concentration in the blood can be approximated in the extracellular space in the liver. Assuming rapid equilibrium between the blood and hepatocytes, the unbound concentration in the blood was used for further analysis. The mean pharmacokinetic parameters of DX-619 were cited from Ref (12). The differential equation was numerically solved to simulate active CYP3A4 content in the liver (E_{act}) using software WinNonlin Professional ver 5.0 and the compiled model (2 compartment IV-Infusion, micro-constants, no lag time, 1st order elimination) when DX-619 (1200 mg=2989 μmol, 2 h infusion) was assumed to be intravenously administered for 15 days (Day 1, Day 3–15). k_{deg} has been cited from previous reports; 0.000481 min^{-1} (15), 0.000321 min^{-1} (16) and 0.000136 $min.^{-1}$ (17)

Cell Culture and *In Vitro* Transport Studies

HEK293 cells stably expressing hOAT1, hOAT3, hOCT2, hMATE1 and hMATE2-K were established as described previously (18,19). Uptake experiments were performed as described previously (18,20). Mock and MDR1-LLC-PK1 were kindly provided by Dr. Piet Borst (21). Transcellular transport assays were performed as described previously (22). In brief, Medium 199 (Invitrogen, Grand Island, NY) containing 25 mmol/l HEPES were adjusted at pH 7.4 with 0.1 N NaOH and used for transport assay. After preincubation of both sides of Transwell (polycarbonate membrane, 0.4 μm pore size, 24 mm diameter, Corning Inc., Corning, NY) with the transport buffer for 10 min at 37°C, the transport assay was started by adding cortisol (final concentration 1 μmol/l) or 6β-OHF (10 μmol/l) to the apical or basal side of the monolayer. In the acceptor side, the transport buffer contained 4% of BSA. After the cells were incubated for 30, 60, 90 and 120 min, 100 μl of aliquot were taken from the acceptor side, and replaced with the cortisol and 6β-OHF free transport buffer containing 4% of BSA. The inhibitory effect of DX-619 on P-gp mediated cortisol transport was examined. DX-619 was added (1–300 μmol/l) in both donor and acceptor sides of the transwell during the experiments. Transport rates were calculated from the slopes of the time profiles of the apical-to-basal and basal-to-apical transports.

Blood and Urine Specimens from Healthy Subjects

The blood and urine specimens used in this study originated from the phase I study of DX-619 in healthy subjects (eight males and one female) who had received a single dose of DX-619 (given by intravenous infusion of 1,200 mg for 2 h), and then 48 h after the initial dose received multiple dosings (1,200 mg of DX-619 q.d. on day 3–15). The reference product (placebo) used was a saline solution. The blood and urine specimens were sorted at −80°C until analysis. The study protocol and the informed consent forms were approved by MDS Pharma Services (Neptune, NJ) Institutional Review Board. The study was conducted at MDS Pharma Services in compliance with ethical principles that have originated from the Declaration of Helsinki and in accordance with the US FDA guidelines for Good Clinical Practice, and the Guideline for the Monitoring of Clinical Investigations.

Determination of Binding of 6β-OHF in Human Plasma

The unbound fraction of 6β-OHF in three individual human plasma (Biopredic International, Rennes, France) was determined using a rapid equilibrium dialysis method. The assay was performed as described previously (23). Briefly, three separate aliquots of plasma spiked with 6β-OHF (final

concentrations of 50 and 200 nmol/l) were placed into the sample chamber, and PBS was placed in the adjacent chamber. After incubation at 37°C for 6 h on an orbital shaker, 6β-OHF in the aliquot of each chamber was analyzed by LC-MS/MS.

Quantification of DX-619, Cortisol and 6β-OHF in the Biological Samples by LC-MS/MS

Analytes of DX-619 in human plasma were added with internal standard solution (d_3-DX-619), isolated thorough solid phase extraction using Oasis HLB 96-well SPE cartridges (Waters Corporation, Milford, MA) and reconstituted in formic acid/acetonitrile (75:25, v/v) solution. Analytes of DX-619 in human urine were diluted with an addition of formic acid/acetonitrile solution and added with internal standard solution (d_3-DX-619). DX-619 was analyzed on a Shimadzu LC-10 AD HPLC system coupled with API 3000 (Applied Biosystems, Foster City, CA), using an ODS-AQ 5 μm 50× 3.0-mm column (YMC Co., Ltd., Kyoto. Japan). An isocratic elution was carried out at 0.3 ml/min of formic acid/acetonitrile (80:20, v/v). The analysis was carried out in the multiple reaction monitoring (MRM) mode with monitoring of precursor-product ion pairs of m/z 402→384 for DX-619, m/z 405→387 for d_3-DX-619.

For cortisol and 6β-OHF analysis, plasma and urine samples and free fraction of 6β-OHF were added to an internal standard solution (6α-methylprednisolone) and subjected to extraction with ethyl acetate. The organic fractions were evaporated, and reconstituted in water/methanol (4:1, v/v). Cortisol and 6β-OHF were analyzed on an Agilent Technologies HP1100 system (Santa Clara, CA) coupled with API 3000, using a Capcell Pack C_{18} UG120 3 μm 50×2.0-mm column (Shiseido Co., Ltd., Tokyo, Japan) and the mobile phase consisted of solvent A, 10 mM ammonium acetate (pH 6.0); and solvent B, acetonitrile with an A/B gradient of 95:5 (0–2 min), 80:20 (4 min) and 40:60 (5–8 min) at a flow rate of 0.3 ml/min. The analysis was carried out in MRM mode with monitoring of m/z 363→327 for cortisol, m/z 379→325 for 6β-OHF and m/z 375→279 for 6α-methylprednisolone. The calibration curves for cortisol, 6β-OHF and DX-619 were constructed at 1.0–200, 1.0–1000 and 10–5000 ng/ml, respectively. The inter-day variability of each compound was <15%.

Calculation of $CL_{6\beta\text{-OHF}}$ and $CL_{renal,\ 6\beta\text{-OHF}}$

$CL_{6\beta-OHF}$ and $CL_{renal,\ 6\beta-OHF}$ are calculated as follows:

$$CL_{6\beta-OHF} = X_{6\beta-OHF}/AUC_{cortisol} \quad (3)$$

$$CL_{renal,\ 6\beta-OHF} = X_{6\beta-OHF}/AUC_{6\beta-OHF} \quad (4)$$

where $X_{6\beta-OHF}$ is the amount of 6β-OHF excreted into the urine, $AUC_{cortisol}$ and $AUC_{6\beta-OHF}$ is the area under the time-concentration profiles (AUC) of plasma cortisol and 6β-OHF during the designated time intervals.

Effects of DX-619 on 11β-hydroxysteroid Dehydrogenase (11β-HSD) 1 and 11β-HSD 2

HEK293 cells expressing 11β-hydroxysteroid dehydrogenase (11β-HSD) 1 or SF9 cells expressing 11β-HSD2 were established as reported previously (24,25). The cells were homogenated and extracted as microsomal pellets. The pellets were resuspended in 20 mM Tris–HCl (pH 8.0) containing 10% glycerol, 1 mM EDTA and 300 mM NaCl. The 11β-HSD1 enzyme assay was conducted in an assay buffer containing 3.2 mmol/l NADPH, 24 mmol/l D-glucose 6-phosphate, 1.38 U/ml glucose-6-phosphate dehydrogenase, 12 mmol/l $MgCl_2$ and enzyme suspension. The 11β-HSD2 enzyme assay was carried out in an assay buffer containing 170 μmol/l NAD^+ and enzyme suspension. Enzyme reactions were initiated by the addition of substrate (cortisone for 11β-HSD1 and cortisol for 11β-HSD2, 160 nmol/l), and after a 20-min incubation at room temperature, terminated by the addition of 50 mmol/l carbenoxolone. Cortisol concentration was measured with a HTRF cortisol assay (Cisbio Bioassays, Cedex, France).

Statistical Analysis

Statistically significant differences in this study were determined using two-tailed unpaired *t*-tests. Differences were considered to be significant at $P<0.05$ and <0.01.

RESULTS

Mechanism-Based Inhibition of Midazolam 1-hydroxylation *In Vitro* by DX-619 and Simulation of the *In Vivo* CYP3A Activities During DX-619 Administration

Midazolam 1'-hydroxylation in HLM was decreased in the presence of DX-619 (100 μmol/l) to 82.0±6.1% of the control group. Preincubation of HLM in the presence of DX-619 potentiated the inhibition in a preincubation-time and concentration-dependent manner (Fig. 2a) with K_I and k_{inact} of 67.9±7.3 μmol/l and 0.0730±0.0033 min^{-1}, respectively (Fig. 2b). The true K_I, corrected by binding to the HLM, ($f_{u,HLM}$ 0.881±0.014) was 59.8±6.5 μmol/l. The preincubation time dependent inhibition was reproduced in a CYP3A4 supersome (data not shown).

The simulation of active CYP3A4 in the liver was conducted using three different k_{deg} values (0.000481, 0.000321 and 0.000136 min^{-1}) (15–17). DX-619 caused prompt reduction of E_{act} on Day 1 and the reduction reached the maximum

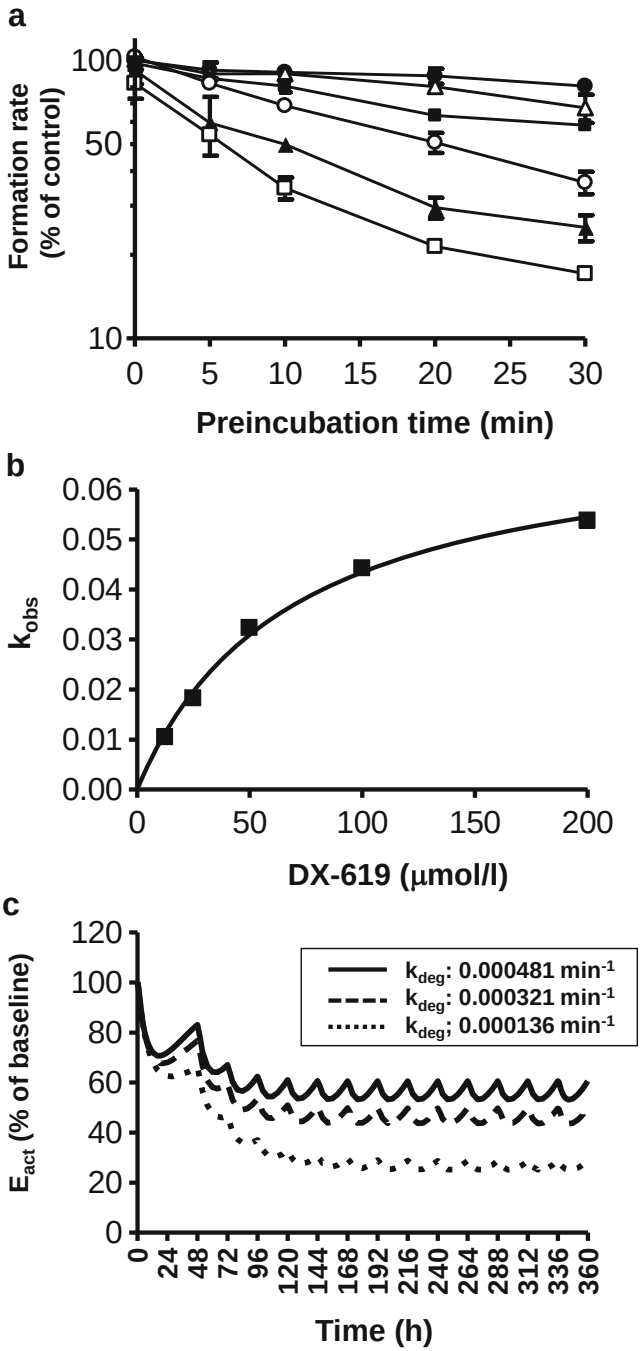

Fig. 2 MBI of CYP3A4 by DX-619 in human liver microsomes and its effect on *in vivo* CYP3A4 activity. (**a**) Midazolam 1'-hydroxylation by HLM (1.0 mg/ml) was determined at 37°C following pre-incubation for the designated time in the presence of various concentrations of DX-619 (μmol/l); ●, 0; Δ, 12.5; ■, 25; ○, 50; ▲, 100; □, 200. Each symbol represents the mean ± S.E. (n=3). (**b**) Concentration dependence of MBI of Midazolam 1'-hydroxylation is shown. The line represents the fitted line. (**c**) E_{act} were simulated using the fitted values, and reported k_{deg} values.

of 53.3% of the control group at 128 h with k_{deg} of 0.000481 min^{-1} used, 43.8% at 152 h with k_{deg} of 0.000321 min^{-1}, and 25.4% at 200 h with k_{deg} of 0.000136 min^{-1}. The simulation predicts a reduction of CYP3A4 activity during DX-619 treatment by 25–53% of the control group (Fig. 2c). Since E_{act} is associated with V_{max}, the intrinsic activity of CYP3A4 is proportional to this value, suggesting *in vivo* relevance of CYP3A4 inhibition by DX-619 during the treatment.

Pharmacokinetic Parameters of Cortisol and 6β-OHF in Placebo and DX-619-Treated Groups

The plasma concentration of cortisol in the placebo group showed a circadian rhythm (Fig. 3, upper). C_{max} of cortisol (2 h) was 2.4-fold higher in the DX-619 treated group compared with the placebo group (P=0.0868). The plasma AUC of cortisol was slightly elevated by DX-619 administration (115% (P=0.0910) and 105% (P=0.4049) on day 1 and 15, respectively), whereas that of 6β-OHF was unaffected by DX-619 (104% (P=0.5167) and 105% (P=0.5059) on day 1 and 15, respectively) (Table 1).

$Xe_{,6\beta-OHF}$ was significantly lower in the DX-619-treated group than that of the placebo group on both day 1 (P<0.05) and day 15 (P<0.01) (Table 1). $CL_{6\beta-OHF}$ was decreased to 1.24±0.12 ml/min (0–24 h, P=0.0546) and 0.684±0.083 ml/min (336-360 h, P<0.01) during DX-619 treatment compared to that of the placebo group as 3.74±1.63 ml/min (0–24 h) and 2.49±0.73 ml/min (336–360 h), respectively (Fig. 4a). $CL_{renal,\ 6\beta-OHF}$ were also significantly decreased to 34.9±3.7 ml/min (0–24 h, P<0.05) and 23.0±3.5 ml/min (336–360 h, P<0.05) during DX-619 treatment compared to that of the placebo group, 84.8±27.3 ml/min (0–24 h) and 78.0±24.3 ml/min (336–360 h), respectively (Fig. 4b). The mean unbound fractions of 6β-OHF were determined *in vitro* in human plasma ($f_{p,\ 6\beta-OHF}$) to be 0.192±0.012 spiked 200 nmol/l of 6β-OHF (as final concentration) and 0.208±0.016 spiked 50 nmol/l of 6β-OHF.

Uptake of cortisol and 6β-OHF by hOAT1-, hOAT3- and hOCT2-HEK

The uptake of the representative substrates, ^{3}H-PAH (50 nmol/l) for hOAT1, ^{3}H-ES (25 nmol/l) for hOAT3 and ^{14}C-TEA (5 μmol/l) for hOCT2 were 5.10±0.074, 6.02±0.28 and 10.2±0.4 μl/min/mg protein, which were all 25-fold higher than that in mock vector transfected cells. Uptake of 6β-OHF was significantly higher in hOAT3- and hOCT2-HEK than in mock cells (Fig. 5a). The uptake by hOAT3 was inhibited by 1 mmol/l probenecid, however, the uptake by hOCT2 was not inhibited by 1 mmol/l quinidine (Fig. 5a). The uptake of 6β-OHF by OAT3 was linear until 5 min (Fig. 5b). The uptake of 6β-OHF by OAT3 was saturable with K_m and V_{max} of 183±25 μmol/l and 782±45 pmol/min/mg protein, respectively (Fig. 5c), and inhibited by DX-619 and probenecid with Ki values of 239±36 and 12.1±3.8 μmol/l

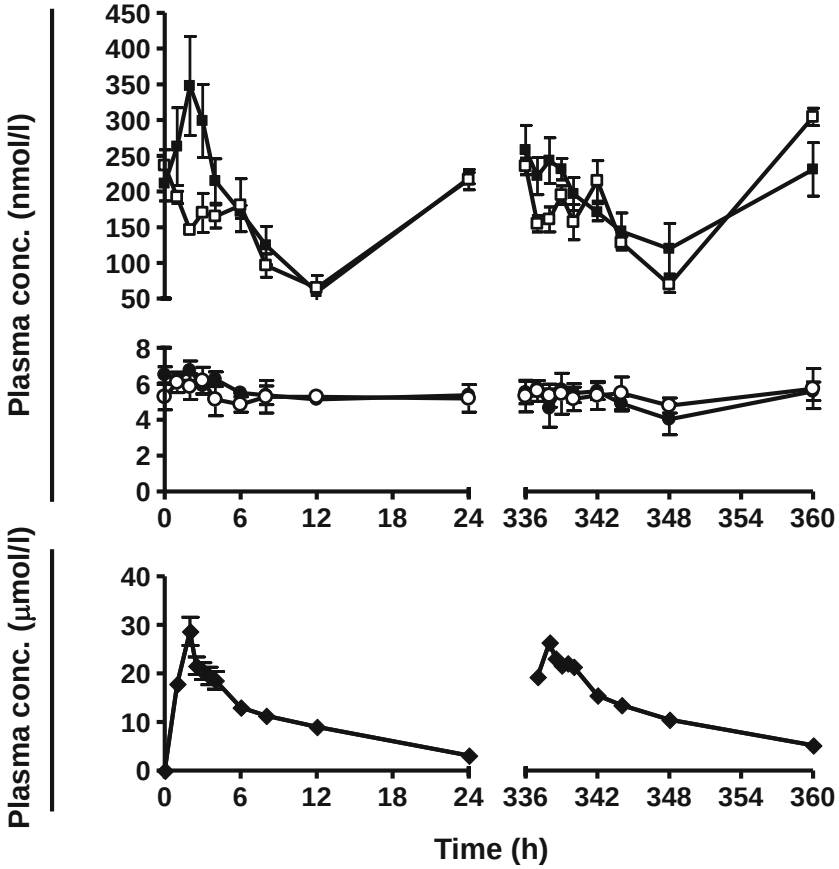

Fig. 3 Plasma concentration-time profiles of cortisol, 6β-OHF and DX-619. Plasma concentrations of cortisol (upper), 6β-OHF (middle) and DX-619 (lower) were determined in the placebo (open symbols) or DX-619 treated groups (closed symbols). Plasma concentration time profile of DX-619 was cited from a previous report (12) for reference. Each point represents the mean ± SE of the six (for DX-619) and three (for placebo) subjects.

(Fig. 5d). The relative contribution of hOAT3 and hOCT2 to uptake in proximal tubule were estimated using the relative activity factor (RAF) method employing ES and TEA as reference compounds.(12,19,26,27) The renal uptake clearance of 6β-OHF mediated by hOAT3 and hOCT2 were predicted to be 0.271 and 0.00890 ml/min/g in the kidney, suggesting the predominant contribution of hOAT3.

Uptake of 6β-OHF by hMATE1- and hMATE2-K-HEK

The uptake of the representative substrate, ^{14}C-TEA by hMATE1- and hMATE2-K-HEK for 1 and 2 min (μl/mg protein) were 22.8±0.6 and 11.2±0.5, which are 97 and 24 times higher than those in mock vector transfected cells ($P<0.01$). The uptake of 6β-OHF by hMATE1- and hMATE2-K HEK was significantly greater than that by mock cells and stimulated by the outward H^+ gradient (Fig. 6a), and pyrimethamine abolished the uptake. The uptake of 6β-OHF by hMATE1 was linear up to 1 min (Fig. 6b). The transport velocity increased along with the substrate concentration by 200 μmol/l, and uptake of ^{14}C-TEA by hMATE1 was inhibited by 33.2±0.5% of control in the presence of 6β-OHF (1 mmol/l). DX-619 and pyrimethamine inhibited the uptake of 6β-OHF by hMATE1 with Ki of 4.32±0.79 and

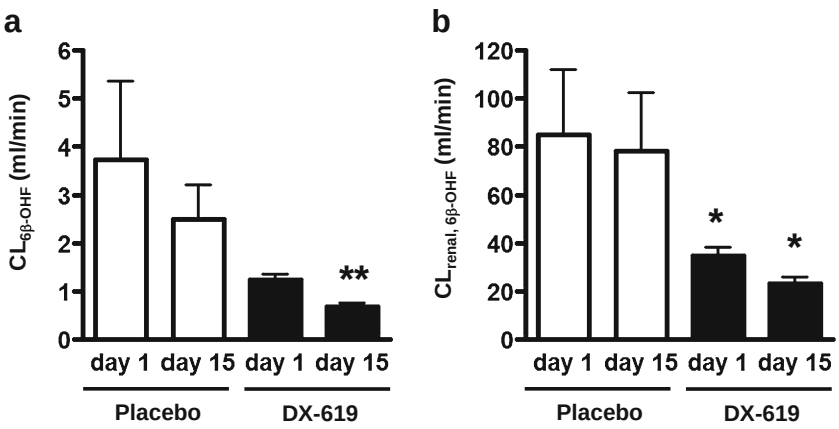

Fig. 4 An index for phenotyping the *in vivo* CYP3A activity ($CL_{6β-OHF}$) and renal clearance of 6β-OHF ($CL_{renal, 6b-OHF}$) during DX-619 treatment. (**a**) $CL_{6β-OHF}$ and (**b**) $CL_{renal, 6β-OHF}$ was calculated in the placebo (open symbols) and DX-619-treated groups (closed symbols). Each point represents the mean ± SE of the six (for DX-619) and three (for placebo) subjects. *, $P<0.05$, **, $P<0.01$ placebo *versus* the DX-619 treated group.

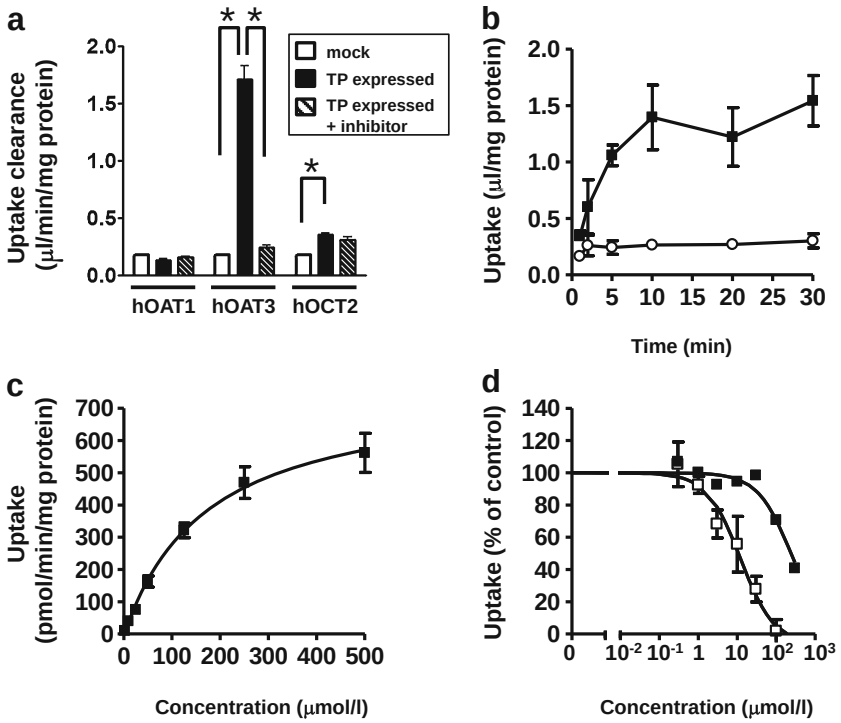

Fig. 5 Uptake of 6β-OHF by OAT1-, OAT3- and OCT2-HEK. (**a**) Uptake of 6β-OHF (5 μmol/l) for 5 min was determined in mock-vector transfected (open bar), and hOAT1-, hOAT3- or hOCT2-HEK (closed bar) at 37°C in the absence and presence of their representative inhibitors (hatched bar, 1 mmol/l; probenecid for hOAT1 and hOAT3, quinidine for hOCT2). * $P < 0.05$ (**b**) Uptake of 6β-OHF (25 μmol/l) by mock-vector transfected (open circles) and hOAT3-HEK (closed square) cells were determined at a designated time point. (**c**, **d**) The uptake of 6β-OHF by hOAT3 for 5 min was determined at various substrate concentrations (2.5–500 μM) (**c**), or in the presence of DX-619 (closed square) or probenecid (open square) at designated concentrations (**d**). The line represents the fitted line obtained by nonlinear regression analysis. Each value represents the mean ± SE of three separate determinations.

0.281±0.033 μmol/l, respectively (Fig. 6c). Transport activities of 6β-OHF by renal transporters, and inhibition potency of DX-619 were summarized in Table 2.

Transcellular Transport of 6β-OHF Across the Monolayers of Mock-Vector Transfected and MDR1-Expressing LLC-PK1

The transcellular transport of 6β-OHF (10 μmol/l) across the monolayers of mock-vector transfected and MDR1-LLC-PK1 was determined in the basal-to-apical and apical-to-basal directions for 120 min at 37°C. Cortisol was used as the representative substrate of P-gp (11). The trancellular transport of cortisol in the basal-to-apical and apical-to-basal direction is identical in mock-vector transfected LLC-PK1 (0.404±0.014 *versus* 0.376±0.003 pmol/min), whereas overexpression of P-gp induced the directional transport; the transport in the basal-to-apical transport was 3.3-fold larger than that in the opposite direction (0.643 ±0.010 *versus* 0.196±0.011 pmol/min). Transport rates of 6β-OHF in the basal-to-apical direction were identical to that in the opposite direction in mock-vector transfected LLC-PK1 (0.248±0.019 *versus* 0.261±0.075 pmol/min). The apical-to-basal and basal-to-apical transport rates of 6β-OHF were 2.0- and 1.5-fold higher in MDR1-LLC-PK1 than the corresponding transport in mock-vector transfected LLC-PK1 ($P<0.05$). The apical-to-basal transport was 1.4-fold greater than that in the opposite direction in MDR1-LLC-PK1. The addition of a potent MDR1 inhibitor, GF120918 (10 μmol/l) to the transport buffer decreased the apical-to-basal transport rate of 6β-OHF in MDR1-LLC-PK1 to the basal-to-apical transport rate, but had no effect on the transcellular transport of 6β-OHF in mock-vector transfected LLC. P-gp mediated directional transport of cortisol was not inhibited by 300 μmol/l of DX-619.

Inhibitory Effects of DX-619 on 11β-HSD1 and 11-β-HSD2 Activities

The effect of DX-619 on 11β-HSD1 and 11β-HSD2 was examined *in vitro* using representative substrates (cortisone for 11β-HSD1, and cortisol for 11β-HSD2). A potent inhibitor of 11β-HSD1 and 11β-HSD2, carbenoxolone, inhibited both enzymes with Ki values of 0.128±0.030 and 0.0147± 0.0030 μmol/l, respectively, which are consistent with previous reports (24,25). DX-619, clarithromycin and itraconazole had no effect on 11β-HSD1 and 11β-HSD2 activities.

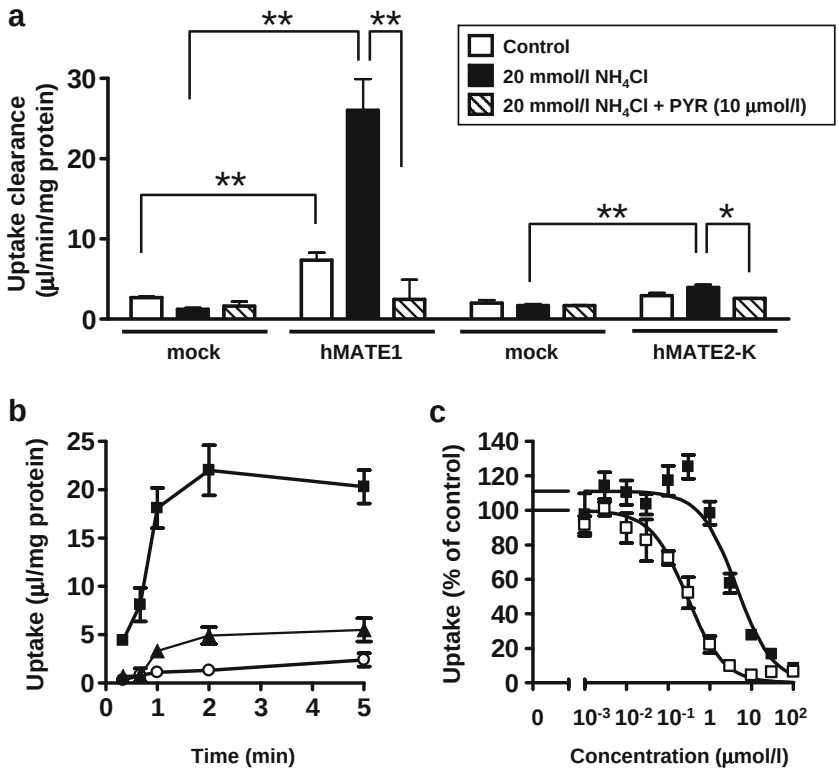

Fig. 6 Uptake of 6β-OHF by hMATE1 and hMATE2-K-HEK. (**a**) Uptake of 6β-OHF (10 μmol/l) was determined in mock-vector transfected and hMATE1 for 1 min and in mock-vector transfected and hMATE2-K-HEK for 2 min, in the presence (closed bar) and absence (open bar) of NH_4Cl (20 mmol/l). In addition to NH_4Cl (20 mmol/l), pyrimethamine (10 μmol/l) was added to inhibit MATEs (*hatched bar*). *, $P < 0.05$, **, $P < 0.01$ (**b**) Uptake of 6β-OHF (10 μmol/l) by mock-vector transfected (open circles), and hMATE1- (closed square) and hMATE2-K-HEK (closed triangle) was determined in the presence of NH_4Cl (20 mmol/l) at the designated time. (**c**) Uptake of 6β-OHF (10 μmol/l) for 1 min by hMATE1-HEK was determined in the presence and absence of DX-619 (closed square) or pyrimethamine (open square). The line represents the fitted line. Each bar or point represents the mean ± SE of three separate determinations.

DISCUSSION

The present study evaluated the mechanism-based inhibition of CYP3A4 by DX-619 using cortisol and 6β-OHF as endogenous biomarkers in healthy subjects, and also examined the effect of DX-619 on the renal clearance of 6β-OHF which involves the tubular secretion by the transporters.

DX-619 shows mechanism-based inhibition of CYP3A4 *in vitro* (Fig. 2a, b), whereas it inhibits neither 11β-HSD1 nor 11β-HSD2, other enzymes involved in cortisol metabolism. Using the kinetic parameters for MBI determine *in vitro* and three different degradation rates of CYP3A4, a magnitude of CYP3A4 inhibition was simulated in healthy subjects during DX-619 treatment; intravenous infusion of 1200 mg DX-619 for 2 h, and then 48 h after the initial dose, multiple dosings (1200 mg of DX-619 q.d. on day 3–15). This suggests *in vivo* relevance of CYP3A4 inhibition by DX-619 during the treatment (Fig. 2c). To support the simulation, $CL_{6\beta-OHF}$ was determined using phase I samples in healthy subjects (Fig. 4a). $CL_{6\beta-OHF}$ in the placebo was similar to the previous report in Japanese subjects (3.71 ml/min) (7,8), but 2~3 fold higher than those in another report by unknown reason (3). DX-619 hardly affects the AUC of cortisol, whereas it significantly decreased the amount of 6β-OHF excreted into the urine in healthy subjects (Table I). Consequently, $CL_{6\beta-OHF}$ was decreased by 66 and 72% on day 1 and 15, respectively, during the DX-619-treatment compared with the placebo group although the difference reached statistical significance on day 15 (Fig. 4a). This is in good agreement with our simulation.

$CL_{6\beta OHF}$ is defined as the following equation using CL_{CYP3A4}, and $CL_{tot,6\beta-OHF}$, which represent the true formation clearance and total body clearance of 6β-OHF, respectively;

$$CL_{6\beta OHF} = \frac{X_{e,6\beta-OHF}}{AUC_{cortisol}} = CL_{CYP3A4} \cdot \frac{CL_{renal,6\beta-OHF}}{CL_{tot,6\beta-OHF}} \quad (5)$$

In regards to $CL_{6\beta OHF}$ as CL_{CYP3A4}, we need the assumption that all of 6β-OHF is cleared renally (i.e., $CL_{tot,6\beta-OHF} = CL_{renal,6\beta-OHF}$). Otherwise, the absolute value of $CL_{6\beta OHF}$ is influenced by the variation of urinary excretion and metabolic pathway by 11β-HSD2 for 6β-OHF. As far as the ratio of $CL_{renal,6\beta-OHF}$ to $CL_{tot,6\beta-OHF}$ not being altered, $CL_{6\beta OHF}$ can be an index to evaluate the variation of hepatic CYP3A4.

Table I Summary of Kinetic Indices of Cortisol and 6β-OHF on Day 1 and Day 15 after the Administration of DX-619 in Healthy Subjects

		$AUC_{cortisol}$ (ng • h/ml)	$AUC_{6\beta-OHF}$ (ng • h/ml)	$Xe_{,\ 6\beta-OHF}$ (μg)	$CL_{6\beta-OHF}$ (ml/min)	$CL_{renal,\ 6\beta-OHF}$ (ml/min)	$f_u \cdot GFR^a$ (ml/min)	$CL_{sec,\ 6\beta-OHF}$ (ml/min)
Placebo	Day 1	1211 ± 206	48.2 ± 4.8	233 ± 59	3.74 ± 1.63	84.8 ± 27.3	20.4	64.4
	Day 15	1472 ± 83	47.9 ± 6.1	212 ± 49	2.49 ± 0.73	78.0 ± 24.3		57.6
DX-619	Day 1	1391 ± 82	49.9 ± 2.9	102 ± 7*	1.24 ± 0.12	34.9 ± 3.7*		14.5
	Day 15	1539 ± 115	45.8 ± 3.2	60.9 ± 5.1**	0.684 ± 0.083**	23.0 ± 3.5*		2.60

Data are taken from Fig. 3. Each value represents the mean ± SE of six (DX-619) and three (placebo) separate determinations. **P value < 0.01 and *P value < 0.05 compared to the placebo group in the same time interval. $AUC_{cortisol}$, area under the time-concentration profiles (AUC) of plasma cortisol from zero time to 24 h; $AUC_{6\beta-OHF}$, AUC of plasma 6β-OHF from zero time to 24 h; $Xe_{,\ 6\beta-OHF}$, amount of 6β-OHF excreted into the urine from zero time to 24 h. [a] GFR was reported to be 98 (ml/min) (12)

The contribution of the urinary excretion of 6β-OHF to the elimination from the systemic circulation remains unknown. We confirmed absence of interaction of DX-619 with 11β-HSD1 and 11β-HSD2 *in vitro*. Then, we investigated the urinary excretion mechanism of 6β-OHF in the subjects. Considering the unbound fraction of 6β-OHF in human plasma, its renal clearance exceeds the glomerular filtration rate ($f_{p,} \cdot GFR$, 19–20 ml/min) when 98 ml/min (12) was used as GFR, indicating a significant contribution of the tubular secretion involving transporters (Table I). During DX-619 treatment, $CL_{renal,\ 6\beta-OHF}$ was significantly decreased compared with that in the placebo group (Fig. 4b). Since $CL_{renal,\ 6\beta-OHF}$ was similar to its glomerular filtration rate in the DX-619 treated group, the tubular secretion of 6β-OHF was completely inhibited (Table I). Whether this interaction is crucial for the evaluation of hepatic CYP3A4 inhibition using $CL_{6\beta-OHF}$ as the index depends on the significance of renal elimination to the elimination pathway of 6β-OHF from the systemic circulation. When the renal elimination is a predominant pathway, the interaction is not crucial since the amount of 6β-OHF excreted into the urine does not change irrespective of the tubular secretion inhibition. In this case, the interaction should be accompanied with plasma 6β-OHF elevation along with the reduction in $CL_{renal,\ 6\beta-OHF}$, and thus, absence of such effect (Fig. 3) indicates an inhibition of 6β-OHF production. Otherwise, the interaction reduces the amount of 6β-OHF excreted into the urine along with the inhibition of the tubular secretion, and consequently, lowering $CL_{6\beta-OHF}$ and exaggerating hepatic CYP3A4 inhibition. Based on the simulation of active CYP3A4 during the treatment (Fig. 2c), we consider that the reduction in $CL_{6\beta-OHF}$ by DX-619 is attributable to hepatic CYP3A4 inhibition. The present study suggests caution in the evaluation of hepatic CYP3A4 activity using cortisol and 6β-OHF as biomarkers; $CL_{6\beta-OHF}$ may be influenced by the variation in $CL_{renal,\ 6\beta-OHF}$ as well as an additional metabolic pathway during the interaction study. It is strongly recommended to determine $CL_{renal,\ 6\beta-OHF,}$ to evaluate the effect of test drugs and new chemical entities on the renal elimination of 6β-OHF simultaneously. Unless $CL_{renal,\ 6\beta-OHF}$ is significantly decreased, reduction in $CL_{6\beta-OHF}$ will supports the hepatic CYP3A4 inhibition. When the significant reduction of $CL_{renal,\ 6\beta-OHF}$ is observed, it is now critical that there is no method applicable to correct $Xe_{6\beta-OHF}$ without evaluating $CL_{tot,6\beta-OHF}$. Pharmacokinetic interaction studies with transporter inhibitors which do not interact with CYP3A4 are necessary to elucidate the impact of reduction of $CL_{renal,\ 6\beta-OHF}$ on $CL_{6\beta-OHF}$. Recently, Peng *et al.* reported that apparent formation

Table II Transport Activities of 6β-OHF by Renal Drug Transporters, and Inhibition Potency of DX-619

Renal transporters		6β-OHF transport activities	Ki (μmol/l) of DX-619	$I_{u,max}/K_i$
Basolateral side	OAT1	n.t.	930 ± 184[b]	0.009–0.014
	OAT3	+++ (K_m 183 ± 25 μmol/l)	239 ± 36	0.0346–0.0548
	OCT2	+ [a]	0.94[b]	8.79–13.9
Apical side	P-gp	n.t.	> 300 μmol/l	–
	MATE1	+++ (K_m >200 μmol/l)	4.32 ± 0.79	1.9–3.0
			0.82 ± 0.14[b]	10.1–16.0
	MATE2-K	+	0.10 ± 0.01[b]	82.6–131

n.t. not transported,

Data are taken from Figs. 5 and 6. $I_{u,max}$ represents the maximum unbound concentration when DX-619 was given intravenously (1,200 mg)

[a] the uptake was not inhibited by quinidine (1 mM), [b] cited from (12)

clearance of 6β-hydroxycortisone from cortisone can be an alternative hepatic CYP3A4 index, although the sensitivity is lower compared with $CL_{6\beta-OHF}$ in the interaction study, where itraconazole was administered to inhibit CYP3A4 by unknown reason. It is possible that the urinary excretion of 6β-hydroxycortisone is not influenced by the pharmacokinetic interaction in the renal transporters. This must also be examined in future studies.

To provide an insight into the transporters involved in the tubular secretion of 6β-OHF, an *in vitro* transport study was conducted. Relative contribution calculated using the RAF method suggests that hOAT3 makes a far larger contribution than OCT2 in the basolateral uptake of 6β-OHF. Furthermore, 6β-OHF turned out as a substrate of H^+/organic cation exchangers, MATE1 and MATE2-K (Fig. 6), which can secrete cationic drugs across the BBM into the urine with an exchange of H^+, the gradient formed by the Na/H^+ exchanger (28). Since the uptake of 6β-OHF by hMATE1 was linear up to 200 μmol/l, and the uptake of ^{14}C-TEA by hMATE1 was inhibited by at most 50% in the presence of 1 mM 6β-OHF, 6β-OHF is a low affinity substrate of MATE1 (Table II). P-glycoprotein, another apical efflux transporter in the kidney, mediates the efflux of cortisol across the plasma membrane (11), however, 6β-OHF was not transported by P-gp (Table II). It is most likely that the tubular secretion of 6β-OHF in the kidney is mediated by OAT3 and MATEs. We reported that DX-619 is able to inhibit OCT2 and MATEs, but not OAT3, at the doses employed in the phase I study (12). The Ki value of DX-619 for MATE1-mediated 6β-OHF transport was 5-fold greater than the previously reported value (0.8 μmol/l obtained using TEA as test substrate (12)). However, this is still below the circulated maximum free concentration (8.26–13.1 μmol/l), suggesting that DX-619 can inhibit MATE1-mediated transport of 6β-OHF under assumption that the unbound concentration of DX-619 in the kidney to be that in the plasma. Together with clinical data, inhibition of MATEs is likely the mechanism underlying the inhibition of renal elimination of 6β-OHF by DX-619 (Table II). Inhibitors for OAT3 and MATEs, which do not interact with CYP3A4, will elucidate the impact of inhibition of the renal elimination of 6β-OHF on $CL_{6\beta-OHF}$.

In the pharmaceutical industries, many drug candidates sometimes have MBI-based DDI potential in unavoidable circumstances considering their DDI risks and clinical benefits. We need clinical data on the magnitude of DDI with victim drugs as early as possible to help decide on candidates for further development. Endogenous compounds have advantage in their capability to suggest *in vivo* relevance of DDIs without administration of probe drugs. However, we need careful consideration on the disadvantage in endogenous compounds such as circadian rhythm, homeostasis, inter- and intra-individual variations, lack of data on the metabolism and elimination pathways, and unforeseen pharmacokinetic interaction. In the present study, we clarified that the urinary excretion of 6β-OHF in human kidney involves tubular secretion where OAT3 and MATEs are candidate transporters. Particularly, DX-619 inhibits MATEs, which may also reduce $CL_{6\beta-OHF}$.

In conclusion, DX-619 is a mechanism-based inhibitor of CYP3A4 *in vitro*. DX-619 treatment caused a moderate inhibition of hepatic CYP3A4-mediated formation, and a significant inhibition of MATE-mediated efflux, of 6β-hydroxycortisol into the urine. This study suggests caution in applying $CL_{6\beta-OHF}$ as index for hepatic CYP3A4 activity without evaluating the $CL_{renal,\ 6\beta-OHF}$.

ACKNOWLEDGMENTS AND DISCLOSURES

The authors acknowledge Ryo Atsumi, for his contribution to the study design and interpretation of results.

Yuichiro Imamura, Nobuyuki Murayama, Noriko Okudaira, Ryo Atsumi, Atsushi Kurihara and Takashi Izumi are employees of Daiichi Sankyo Co., Ltd. Other authors declare no conflict of interest.

The study was sponsored by Daiichi-Sankyo Co., Ltd, Tokyo, Japan. This study was also supported by the Japan Health Sciences Foundation [Grants-in-Aid for Public-private sector joint research on Publicly Essential Drugs (KHB 1208)].

REFERENCES

1. Honig PK, Wortham DC, Zamani K, Conner DP, Mullin JC, Cantilena LR. Terfenadine-ketoconazole interaction. Pharmacokinetic and electrocardiographic consequences. JAMA. 1993;269:1513–8.
2. Abel SM, Maggs JL, Back DJ, Park BK. Cortisol metabolism by human liver *in vitro*–I. Metabolite identification and inter-individual variability. J Steroid Biochem Mol Biol. 1992;43:713–9.
3. Peng CC, Templeton I, Thummel KE, Davis C, Kunze KL, Isoherranen N. Evaluation of 6beta-Hydroxycortisol, 6beta-Hydroxycortisone, and a Combination of the Two as Endogenous Probes for Inhibition of CYP3A4 *In Vivo*. Clin Pharmacol Ther. 2011;89:888–95.
4. de Wildt SN, Kearns GL, Leeder JS, van den Anker JN. Cytochrome P450 3A: ontogeny and drug disposition. Clin Pharmacokinet. 1999;37:485–505.
5. Saenger P. 6 beta-hydroxycortisol in random urine samples as an indicator of enzyme induction. Clin Pharmacol Ther. 1983;34:818–21.
6. Bienvenu T, Rey E, Pons G, d'Athis P, Olive G. A simple non-invasive procedure for the investigation of cytochrome P-450 IIIA dependent enzymes in humans. Int J Clin Pharmacol Ther Toxicol. 1991;29:441–5.
7. Furuta T, Suzuki A, Mori C, Shibasaki H, Yokokawa A, Kasuya Y. Evidence for the validity of cortisol 6 beta-hydroxylation

clearance as a new index for *in vivo* cytochrome P450 3A phenotyping in humans. Drug Metab Dispos. 2003;31:1283–7.
8. Ushiama H, Echizen H, Nachi S, Ohnishi A. Dose-dependent inhibition of CYP3A activity by clarithromycin during Helicobacter pylori eradication therapy assessed by changes in plasma lansoprazole levels and partial cortisol clearance to 6beta-hydroxycortisol. Clin Pharmacol Ther. 2002;72:33–43.
9. Fujikawa K, Chiba M, Tanaka M, Sato K. *In vitro* antibacterial activity of DX-619, a novel des-fluoro(6) quinolone. Antimicrob Agents Chemother. 2005;49:3040–5.
10. Asif AR, Steffgen J, Metten M, Grunewald RW, Muller GA, Bahn A, *et al.* Presence of organic anion transporters 3 (OAT3) and 4 (OAT4) in human adrenocortical cells. Pflugers Arch. 2005;450:88–95.
11. Ueda K, Okamura N, Hirai M, Tanigawara Y, Saeki T, Kioka N, *et al.* Human P-glycoprotein transports cortisol, aldosterone, and dexamethasone, but not progesterone. J Biol Chem. 1992;267:24248–52.
12. Imamura Y, Murayama N, Okudaira N, Kurihara A, Okazaki O, Izumi T, *et al.* Prediction of fluoroquinolone-induced elevation in serum creatinine levels: a case of drug-endogenous substance interaction involving the inhibition of renal secretion. Clin Pharmacol Ther. 2011;89:81–8.
13. Watanabe A, Nakamura K, Okudaira N, Okazaki O, Sudo K. Risk assessment for drug-drug interaction caused by metabolism-based inhibition of CYP3A using automated *in vitro* assay systems and its application in the early drug discovery process. Drug Metab Dispos. 2007;35:1232–8.
14. Kanamitsu S, Ito K, Green CE, Tyson CA, Shimada N, Sugiyama Y. Prediction of *in vivo* interaction between triazolam and erythromycin based on *in vitro* studies using human liver microsomes and recombinant human CYP3A4. Pharm Res. 2000;17:419–26.
15. Lai AA, Levy RH, Cutler RE. Time-course of interaction between carbamazepine and clonazepam in normal man. Clin Pharmacol Ther. 1978;24:316–23.
16. Fromm MF, Busse D, Kroemer HK, Eichelbaum M. Differential induction of prehepatic and hepatic metabolism of verapamil by rifampin. Hepatology. 1996;24:796–801.
17. Hsu A, Granneman GR, Witt G, Locke C, Denissen J, Molla A, *et al.* Multiple-dose pharmacokinetics of ritonavir in human immunodeficiency virus-infected subjects. Antimicrob Agents Chemother. 1997;41:898–905.
18. Enomoto A, Takeda M, Taki K, Takayama F, Noshiro R, Niwa T, *et al.* Interactions of human organic anion as well as cation transporters with indoxyl sulfate. Eur J Pharmacol. 2003;466:13–20.
19. Matsushima S, Maeda K, Inoue K, Ohta KY, Yuasa H, Kondo T, *et al.* The inhibition of human multidrug and toxin extrusion 1 is involved in the drug-drug interaction caused by cimetidine. Drug Metab Dispos. 2009;37:555–9.
20. Ohta KY, Imamura Y, Okudaira N, Atsumi R, Inoue K, Yuasa H. Functional characterization of multidrug and toxin extrusion protein 1 as a facilitative transporter for fluoroquinolones. J Pharmacol Exp Ther. 2009;328:628–34.
21. Smith AJ, Mayer U, Schinkel AH, Borst P. Availability of PSC833, a substrate and inhibitor of P-glycoproteins, in various concentrations of serum. J Natl Cancer Inst. 1998;90:1161–6.
22. Kodaira H, Kusuhara H, Ushiki J, Fuse E, Sugiyama Y. Kinetic analysis of the cooperation of P-glycoprotein (P-gp/Abcb1) and breast cancer resistance protein (Bcrp/Abcg2) in limiting the brain and testis penetration of erlotinib, flavopiridol, and mitoxantrone. J Pharmacol Exp Ther. 2010;333:788–96.
23. Waters NJ, Jones R, Williams G, Sohal B. Validation of a rapid equilibrium dialysis approach for the measurement of plasma protein binding. J Pharm Sci. 2008;97:4586–95.
24. Cho YS, Kim CH, Cheon HG. Cell-based assay for screening 11beta-hydroxysteroid dehydrogenase 1 inhibitors. Anal Biochem. 2009;392:110–6.
25. Brown RW, Chapman KE, Kotelevtsev Y, Yau JL, Lindsay RS, Brett L, *et al.* Cloning and production of antisera to human placental 11 beta-hydroxysteroid dehydrogenase type 2. Biochem J. 1996;313(Pt 3):1007–17.
26. Hasegawa M, Kusuhara H, Endou H, Sugiyama Y. Contribution of organic anion transporters to the renal uptake of anionic compounds and nucleoside derivatives in rat. J Pharmacol Exp Ther. 2003;305:1087–97.
27. Nozaki Y, Kusuhara H, Kondo T, Hasegawa M, Shiroyanagi Y, Nakazawa H, *et al.* Characterization of the uptake of organic anion transporter (OAT) 1 and OAT3 substrates by human kidney slices. J Pharmacol Exp Ther. 2007;321:362–9.
28. Otsuka M, Matsumoto T, Morimoto R, Arioka S, Omote H, Moriyama Y. A human transporter protein that mediates the final excretion step for toxic organic cations. Proc Natl Acad Sci U S A. 2005;102:17923–8.